Research in Astron. Astrophys. **2013** Vol. **13** No. **3**, 253–258
http://www.raa-journal.org *http://www.iop.org/journals/raa*

Research in Astronomy and Astrophysics

LETTERS

Twist in a polar blowout jet *

Jun-Chao Hong[1,2], Yun-Chun Jiang[1], Jia-Yan Yang[1], Rui-Sheng Zheng[1], Yi Bi[1], Hai-Dong Li[1], Bo Yang[1,2] and Dan Yang[1,2]

[1] National Astronomical Observatories / Yunnan Astronomical Observatory, Chinese Academy of Sciences, Kunming 650011, China; *hjcsolar@ynao.ac.cn*
[2] Graduate University of Chinese Academy of Sciences, Beijing 100049, China

Received 2012 August 16; accepted 2012 December 25

Abstract It is well known that some coronal jets exhibit helical structures and untwisting. We attempt to inspect the origin of twist in a blowout jet. By means of multi-wavelength and multi-angle observations from *Solar Dynamics Observatory* (*SDO*) and *Solar Terrestrial Relations Observatory-Ahead* (*STEREO-A*), we firstly report a polar untwisting jet that is a blowout jet which leads to a jet-like coronal mass ejection. From the viewpoint of *SDO*, the jet shows clear untwisting behavior and two jet-spires. However, from the viewpoint of *STEREO-A* the jet actually comes from the whip-like prominence eruption and is followed by a white-light jet. Our observations indicate that twist in blowout jets may result from the erupting mini-prominences/mini-filaments in the jet base.

Key words: Sun: corona — Sun: coronal mass ejections — Sun: prominences

1 INTRODUCTION

Coronal jets are collimated transient ejections of plasma occurring almost everywhere over the solar surface. They were discovered with the Soft X-ray Telescope on *Yohkoh* (Shibata et al. 1997). The term, coronal jets, describes a wide range of temperatures in plasma ejections including Hα surges, ultraviolet (UV) jets, extreme-ultraviolet (EUV) jets, soft X-ray jets and white light jets (e.g., Schmieder et al. 1994; Chen et al. 2008; Chifor et al. 2008a,b; Yang et al. 2011; Tian et al. 2011; Zhang et al. 2000; Moore et al. 2011; Wang et al. 1998). The basic driving mechanism behind various jets involves magnetic reconnection where the emerging magnetic flux interacts with a high ambient unipolar field (e.g., the 2D simulations, Yokoyama & Shibata 1996).

Coronal jets have on occasion exhibited helical structure and untwisting motion (e.g., Canfield et al. 1996; Alexander & Fletcher 1999; Harrison et al. 2001; Jibben & Canfield 2004). Patsourakos et al. (2008) used Solar Terrestrial Relations Observatory (*STEREO*)/EUVI (Wuelser et al. 2004) images to determine the three-dimensional topology of a polar jet, clearly demonstrating the twisted structure. Nisticò et al. (2009) carried out a statistical study of coronal jets using EUVI observations of 79 events and found that among 61 characterized events, 31 ($\sim$50%) showed untwisting behavior. Recently, Shen et al. (2011) and Chen et al. (2012) presented a detailed study of the same untwisting jet with high temporal and spatial observations taken by *Solar Dynamics Observatory*

* Supported by the National Natural Science Foundation of China.

(*SDO*)/Atmospheric Imaging Assembly telescope (AIA; Lemen et al. 2012). The basic interpretation for these observations is that the emerging flux in the jet base contains twisted field lines, allowing for helicity transfer to the reconnected open field via interchange reconnection, which was demonstrated in recent jet simulations (Moreno-Insertis et al. 2008; Pariat et al. 2009, 2010).

On the other hand, Moore et al. (2010) suggest that jets can be grouped into two categories, namely standard jets and blowout jets. Standard jets fit the emerging flux-open field reconnection model mentioned above, and mainly exhibit one bright spire in X-rays. However, blowout jets fit a picture where the jet-base magnetic arch, often carrying a filament, has enough magnetic shear and twist to undergo a miniature version of a blowout eruption that produces a major coronal mass ejection (CME), thus exhibiting multiple spires with material from the chromosphere and transition region ejected in EUV emissions. Previous studies did not examine whether the observed untwisting jets belong to a standard type or a blowout type. We consider that the twist in blowout jets may result from a small erupting filament field, while the twist in standard jets is derived from the emerging flux. Liu et al. (2011) identified an EUV blowout jet whose spire exhibited untwisting motion but no filament in the jet base was seen. In Hong et al. (2011), we reported a blowout jet caused by a mini-filament eruption but no untwisting behavior was observed. Other observations on blowout jets (e.g. Yang et al. 2012; Shen et al. 2012) also did not point to the relationship between the untwisting motion of the jet and the jet-base filament. In this paper, using multi-angle observations we inspect this relationship with a polar blowout jet which displayed clear untwisting motion when its base prominence underwent a whipping-like eruption.

2 OBSERVATIONS

On 2011 April 22, a jet was observed near the northern pole of the Sun by *SDO*/AIA and *STEREO-Ahead (STEREO-A)*. AIA captures full-disk images of the Sun's atmosphere out to 1.3 solar radii in seven EUV and three UV-visible wavebands, with a pixel size of $0.6''$ and a cadence of 12 (24) s for EUV (UV). We focus on the 304 Å (He II; $\log T = 4.7$) and 171 Å (Fe IX; $\log T = 5.8$) images because the event is clearer in these two filters. *STEREO A* detected the jet from the other viewpoint with an angle of about 90° ahead the Earth (or *SDO*). We examine full-disk *STEREO*/EUVI images, with a field of view (FOV) out to about 1.7 solar radii and a pixel resolution of $1.6''$. The images have a time cadence of 10 min in 304 Å and 2.5 min in 195 Å. Coronagraphy observations from *STEREO A*/COR1 (Thompson et al. 2010) are also utilized to identify the associated CME. COR1 A recorded the white-light images which have an FOV from 1.5 to 4 solar radii, with a pixel resolution of $15''$ and a 5-minute cadence for our event.

3 RESULTS

The general evolution of the polar jet is shown in Figure 1. According to the AIA 304 Å observation, the jet was close to the solar limb, starting at about 04:50 UT and ending around 05:20 UT. As a collection of plasma rising above the surrounding spicular material, the jet was formed as a wide upward structure. Beginning from 04:55 UT, brighter plasma started to travel along the edges of the jet, indicated by the arrows in Figure 1(b)–(d), which appeared to highlight twisted magnetic field lines and thus led to the jet displaying an upward helical body. As the whole helical body was rising higher, we note that a moving bright feature (MBF indicated by the radial arrows) rotated and unwound around the axis of the jet. We also tracked the MBF from 04:55:06 UT to 04:59:08 UT and overlaid the tracks on the AIA 304 Å image at 05:01:32 UT. The tracks of the bright feature display a projection of a three-dimensional spiral motion. These phenomena suggest that the polar jet untwisted itself when rising. By examining a movie of the AIA 304 Å event, it is clear that the jet spun counterclockwise as viewed from its base during 04:55–05:02 UT. So, the untwisting jet is a left-handed jet according to the definition of chirality for jets in Jibben & Canfield (2004). In addition, the jet has a different appearance in the higher temperature filters of AIA. The AIA 171 Å

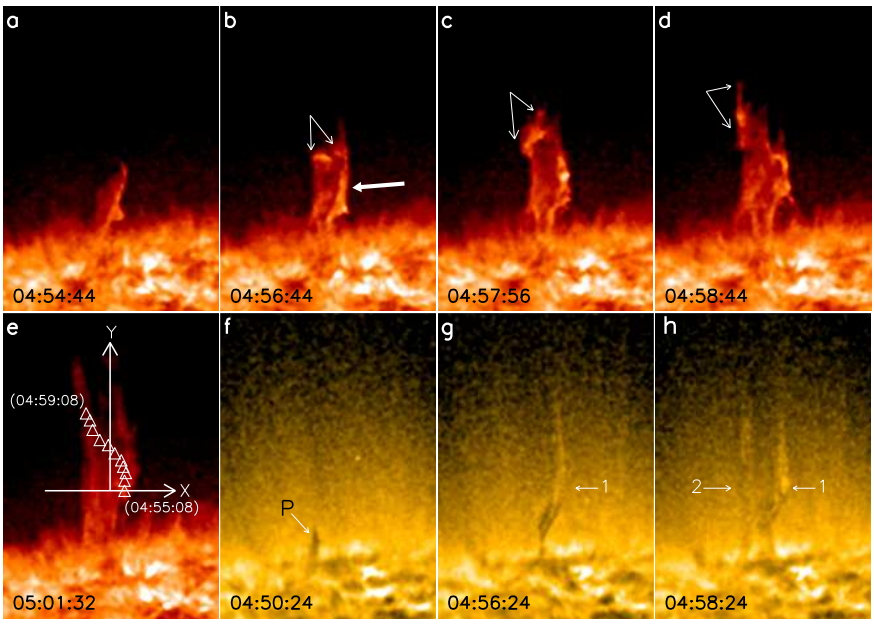

Fig. 1 *SDO*/AIA 304 Å (a–e) and 171 Å (f–h) images showing the jet eruption. The thick arrow in panel (b) shows the twisted magnetic field highlighted by bright plasmas. The radial arrows in panels (b)–(d) point to the MBFs. The triangles overlaid on panel (e) are the tracks of MBFs from 04:55:08 to 04:59:08 UT. Two perpendicular coordinate axes labeled with X and Y are also plotted in panel (e), and are used as a coordinate system for Fig. 2. The FOV is $100'' \times 145''$.

images in Figure 1 show that the jet began as a protrusion of cool plasma, 'P,' and then grew into one threadlike spire denoted by '1,' which was different from the wide body in the 304 Å. Interestingly, an extra jet-spire denoted by '2,' appeared close to the spire '1.' This may indicate that we observed a polar blowout jet, as suggested by Moore et al. (2010). However, none of the AIA filters gave clear observations of the jet-base arch due to the jet actually shooting up from behind the solar limb in the view of *SDO* and the base arch might have plasma beyond the temperatures that generate EUV emissions.

To reveal the kinematics of the jet more clearly, we examined the time profiles of the location coordinates of the tracked MBFs and illustrated the results in Figure 2. The coordinates were measured in the coordinate system shown in Figure 1(e). The origin of the coordinate system is from the average x value over 04:55:08–04:59:08 UT and the initial y value at 04:55:08 UT, respectively as measured from the tracks of the MBF. The X components (diamonds) of the coordinates represent the transverse lengths across the jet as locations of the MBFs relative to the Y axis, while the Y components (asterisks) represent the vertical/axial heights of the MBFs along the jet relative to the X axis. According to the distributions of the two components in Figure 2, we can see that the MBFs seemed to make a circular motion around the jet while moving at an approximately constant speed along the jet's axis. We performed a trigonometric fitting to the transverse lengths and a linear fitting to the axial heights. The fitting functions are $x = 9.845 \times \sin(0.013 \times t + 3.742) - 2.421$ and $y = -40.3 + 0.148 \times t$, where x and y are in units of arcsecs, and t is the time in seconds. So, the rotation period (T), angular speed (w), rotation radius (r), transverse velocity ($v_{\rm t}$) and axial velocity ($v_{\rm a}$) of MBFs are derived and shown in the corresponding panel of Figure 2. The values of T, w, r, $v_{\rm t}$ and $v_{\rm a}$ are 475 s, 0.76° s^{-1}, 7.2 Mm, 95 km s^{-1} and 108 km s^{-1}, respectively. The twist stored in the jet can further be estimated by multiplying w by the duration of untwisting for the jet ($\sim$7 min).

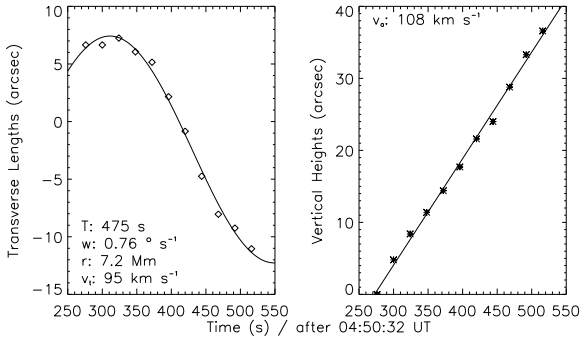

Fig. 2 Time variations of the location coordinates (represented by the diamonds and asterisks) of MBFs in arcsecs. Their positions are measured in the coordinate system shown in Fig. 1 (e) with its origin at (–115.435, 985.815). Left panel shows the evolution of transverse lengths from the X component (east-west direction) of the coordinates. Right panel shows the evolution of the vertical heights from the Y component (south-north direction) of the coordinates. The solid lines are the results of trigonometric and linear fittings to the transverse and axial heights, respectively. T, w, r, $v_{\rm t}$ and $v_{\rm a}$ represent the rotation period, rotation speed, rotation radius, transverse velocity and axial velocity of MBFs, respectively.

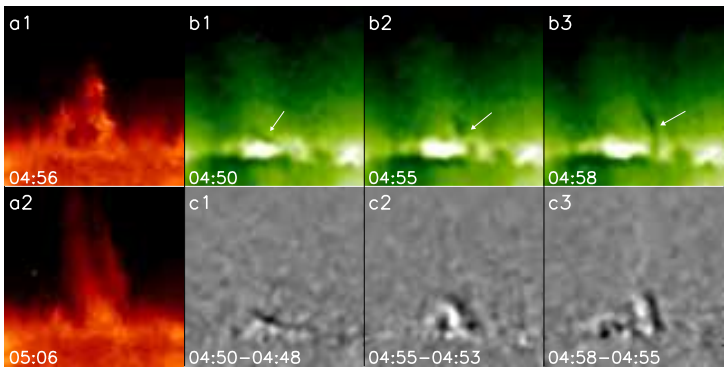

Fig. 3 *STEREO A*/EUVI 304 Å direct (a1–a2) and 195 Å direct (b1–b3) and running-difference (c1–c3) images, showing the whiplike prominence eruption. The FOV is $126'' \times 126''$.

The deduced twist is about 0.89 turns or 1.77 π, which means the polar jet untwists itself about one round during the eruption.

From the viewpoint of *STEREO-A*, the polar jet displayed the inherent feature. The results are shown in Figure 3. In the EUVI 304 Å direct images (a1–a2), the jet appeared as an erupting loop-like prominence at 04:56 UT and then ejected into a collimated structure with two legs at 05:06 UT. Therefore, we confirm that this polar jet is indeed a blowout EUV jet, as suggested by Moore et al. (2010). In addition, it is easy to imagine that the untwisting body of the jet detected in AIA 304 Å images actually corresponds to the eruptive prominence itself. Therefore, the twist within the blowout jet originates from the prominence field. Due to their cadence limit, we cannot check the eruption process of the prominence in EUVI 304 Å images. Fortunately, the EUVI 195 Å observations covered the eruption better due to their higher cadence. From the 195 Å direct (b1–b3) and difference (c1–c3) images in Figure 3, the prominence appeared as a small cool arch that rose up from 04:50 to 04:58 UT when its eastern leg apparently disconnected from the solar surface but the western one was still anchored. In such a sequence, the prominence underwent a whiplike eruption as observed

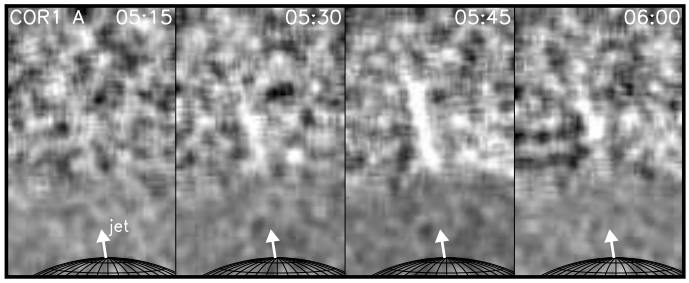

Fig. 4 *STEREO A*/COR1 base-difference images showing the white-light jet directly above the EUV jet indicated by the arrows. The FOV is $1000'' \times 1600''$.

in some mini- or large-scale filament eruptions (Wang et al. 2000; Liu et al. 2009). Meanwhile, the twist stored in the blowout jet or the prominence was released.

The polar blowout jet also led to a jet-like CME, which is similar to the result in Hong et al. (2011). By examining the *STEREO-A*/COR1 white-light observations, a jet-like CME or a coronal white-light jet (Wang & Sheeley 2002; Paraschiv et al. 2010) appeared directly above the jet from 05:30 UT. Due to the close temporal and spatial connection, we believe that the white-light jet originated from the outward extension of the blowout EUV jet.

4 CONCLUSIONS AND DISCUSSION

By analyzing observations with multiple viewpoints from *SDO* and *STEREO-A*, a polar untwisting jet is identified as a blowout EUV jet that comes from the eruption of a prominence. In the *SDO* views, the small jet exhibits untwisting behavior in 304 Å and two jet-spires in 171 Å. By tracking a bright feature moving helically in the jet, we find that the jet untwists itself in a period of 475 s with a rotational speed of 0.76° s^{-1}, and is ejected upward at an approximately constant velocity ($\sim$108 km s^{-1}). Considering that the blowout jet untwists in about 7 min, we also estimated that the twist completes about 0.89 turns. *STEREO* observations further suggest that the blowout jet is indeed a whiplike prominence eruption and leads to a white-light jet. Blowout jets associated with micro CMEs have already been reported in several observations (Hong et al. 2011; Yang et al. 2012; Shen et al. 2012). It is necessary to inspect a general relationship between blowout jets and micro-CME events.

In general, prominences/filaments contain a twisted flux rope after the onset of the eruption. The blowout jet displays untwisting such that its twist directly originates from the prominence and is released by the whiplike eruption of the prominence. During the eruption of the blowout jet, it is expected that the whipping motion would stretch the overlying field loops with a current sheet forming underneath the prominence, where reconnection called "tether release" may occur (Klimchuk 2001). Thus, the twist within the blowout jet/prominence may be released by such a reconnection. Previous studies suggest that the twist in jets often comes from the newly emerging flux and is released by an interchange reconnection with an ambient open field (Canfield et al. 1996; Pariat et al. 2009). Such a scene tends to occur in standard jets without the involvement of filament/prominence eruptions. Therefore, the source and the release of the twist within blowout jets may be generally different from standard jets and be controlled by magnetic fields from their base prominences. If so, we expect that (1) there would be a one-to-one relationship between blowout jet handedness (Jibben & Canfield 2004) and prominence handedness (Martin et al. 1994), which means a left/right-handed blowout jet corresponds to a dextral/sinistral prominence, and (2) the handedness of blowout jets would have a hemispheric preference because of the hemispheric pattern for prominence handedness. The blowout jet presented here is a left-handed jet and thus consistent with the preferential

pattern for a dextral prominence in the northern hemisphere (Zirker et al. 1997). More observations and studies are needed to confirm and clarify these relationships.

Acknowledgements We thank the referee for helpful comments very much. This work is supported by the National Basic Research Program of China (973 Program, 2011CB811403), and by the National Natural Science Foundation of China (Grant Nos. 10973038 and 11173038). The AIA and HMI data used here are courtesy of *SDO* (NASA) and the AIA/HMI consortia. The EUVI and COR1 data are courtesy of the *STEREO* and the SECCHI consortium.

References

Alexander, D., & Fletcher, L. 1999, Sol. Phys., 190, 167
Canfield, R. C., Reardon, K. P., Leka, K. D., et al. 1996, ApJ, 464, 1016
Chen, H. D., Jiang, Y. C., & Ma, S. L. 2008, A&A, 478, 907
Chen, H.-D., Zhang, J., & Ma, S.-L. 2012, RAA (Research in Astronomy and Astrophysics), 12, 573
Chifor, C., Isobe, H., Mason, H. E., et al. 2008a, A&A, 491, 279
Chifor, C., Young, P. R., Isobe, H., et al. 2008b, A&A, 481, L57
Harrison, R. A., Bryans, P., & Bingham, R. 2001, A&A, 379, 324
Hong, J., Jiang, Y., Zheng, R., et al. 2011, ApJ, 738, L20
Jibben, P., & Canfield, R. C. 2004, ApJ, 610, 1129
Klimchuk, J. A. 2001, in Washington DC American Geophysical Union Geophysical Monograph Series, 125, eds. P. Song, H. J. Singer, & G. L. Siscoe (Washington: Am. Geophys. Un.), 143
Lemen, J. R., Title, A. M., Akin, D. J., et al. 2012, Sol. Phys., 275, 17
Liu, R., Alexander, D., & Gilbert, H. R. 2009, ApJ, 691, 1079
Liu, C., Deng, N., Liu, R., et al. 2011, ApJ, 735, L18
Martin, S. F., Bilimoria, R., & Tracadas, P. W. 1994, in Solar Surface Magnetism, eds. R. J. Rutten, & C. J. Schrijver, 303
Moore, R. L., Cirtain, J. W., Sterling, A. C., & Falconer, D. A. 2010, ApJ, 720, 757
Moore, R. L., Sterling, A. C., Cirtain, J. W., & Falconer, D. A. 2011, ApJ, 731, L18
Moreno-Insertis, F., Galsgaard, K., & Ugarte-Urra, I. 2008, ApJ, 673, L211
Nisticò, G., Bothmer, V., Patsourakos, S., & Zimbardo, G. 2009, Sol. Phys., 259, 87
Paraschiv, A. R., Lacatus, D. A., Badescu, T., et al. 2010, Sol. Phys., 264, 365
Pariat, E., Antiochos, S. K., & DeVore, C. R. 2009, ApJ, 691, 61
Pariat, E., Antiochos, S. K., & DeVore, C. R. 2010, ApJ, 714, 1762
Patsourakos, S., Pariat, E., Vourlidas, A., Antiochos, S. K., & Wuelser, J. P. 2008, ApJ, 680, L73
Schmieder, B., Golub, L., & Antiochos, S. K. 1994, ApJ, 425, 326
Shen, Y., Liu, Y., Su, J., & Ibrahim, A. 2011, ApJ, 735, L43
Shen, Y., Liu, Y., Su, J., & Deng, Y. 2012, ApJ, 745, 164
Shibata, K., Shimojo, M., Yokoyama, T., & Ohyama, M. 1997, in ASPC 111, Magnetic Reconnection in the Solar Atmosphere, eds. R. D. Bentley, & J. T. Mariska, 29
Thompson, W. T., Wei, K., Burkepile, J. T., Davila, J. M., & St. Cyr, O. C. 2010, Sol. Phys., 262, 213
Tian, H., McIntosh, S. W., Habbal, S. R., & He, J. 2011, ApJ, 736, 130
Wang, Y.-M., Sheeley, N. R., Jr., Socker, D. G., et al. 1998, ApJ, 508, 899
Wang, J., Li, W., Denker, C., et al. 2000, ApJ, 530, 1071
Wang, Y.-M., & Sheeley, N. R., Jr. 2002, ApJ, 575, 542
Wuelser, J.-P., Lemen, J. R., Tarbell, T. D., et al. 2004, in Society of Photo-Optical Instrumentation Engineers (SPIE) Conference Series, 5171, eds. S. Fineschi, & M. A. Gummin, 111
Yang, L.-H., Jiang, Y.-C., Yang, J.-Y., et al. 2011, RAA (Research in Astronomy and Astrophysics), 11, 1229
Yang, J.-Y., Jiang, Y.-C., Yang, D., et al. 2012, RAA (Research in Astronomy and Astrophysics), 12, 300
Yokoyama, T., & Shibata, K. 1996, PASJ, 48, 353
Zhang, J., Wang, J., & Liu, Y. 2000, A&A, 364, 939
Zirker, J. B., Martin, S. F., Harvey, K., & Gaizauskas, V. 1997, Sol. Phys., 175, 27